

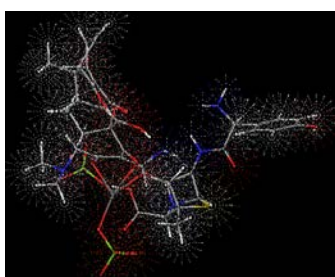
Spectral analysis, XRPD, quantum structures and evaluation of antimicrobial activity of supramolecular topologies of Bi(V) and Co(II) metal based antibiotic drugs complexes

Rajiv Kumar^{1*}, Parashuram Mishra²

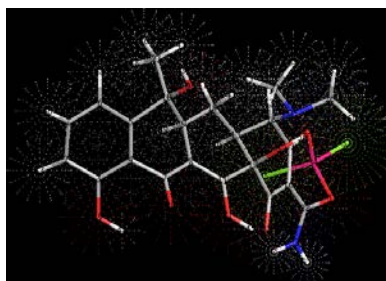
¹University of Delhi, Delhi, India. ²Bioinorganic and Materials Chemistry Research Laboratory, Tribhuvan University, M.M.A.M. Campus, Biratnagar, Nepal.

Received on: 6-July-2016, Accepted and Published on: 7-Sept-2016

ABSTRACT



OMC-Bi(V)



OMC-Co(II)

Supramolecular topologies of organic metal complexes (OMCs) i.e. OMC-Bi(V) and OMC-Co(II) were derived from antibiotic drugs i.e. tetracycline and ampicillin. To find out coordination sites in organic metal complexes(OMCs); therefore, several techniques were used spectral analysis (electronic, vibrational, ¹H NMR, ¹³C NMR, and TOF-MS), physicochemical investigations (elemental analyses, X-ray powder diffraction) and molecular modeling, revealed coordination modes between Bi(V) and Co(II) of L, and ML entirely within moiety OMCs and specifically molecular modeling findings to predict accurately existed bond distance and bond angles. Quantum structures of OMC-Bi(V) and OMC-Co(II) were derived by molecular modeling. The electronic spectrum of OMCs-Bi(V) and OMC-Co(II) showed different transitions corresponding to five and four-coordinate arrangements. XRPD and molecular modeling were also provided information related to fitness of metal and their bonding ability to organic framework and crystal system. XRPD spectral data were used to calculate cell dimension and other parameters lattice parameters for OMC-Bi(V) and OMC-Co(II). OMC-Bi; a = 15.95464 (Å), b = 15.95464 (Å), c = 16.47710 (Å), $\alpha = 90.00^\circ$, $\beta = 90.00^\circ$, $\gamma = 120.00^\circ$ and OMC-Co ; a = 14.27390 (Å), b = 14.27390 (Å), c = 9.51192 (Å), $\alpha = 90.00^\circ$, $\beta = 99.000^\circ$, $\gamma = 120.00^\circ$. Particle size (nm) was also calculated for OMC-Bi(V) and OMC-Co(II) and found 11.66 nm and 10.09 nm respectively. Molecular modeling provided better understanding related to arrangements of atoms in crystal systems. Electron set for bonding groups presented in ligands moieties display extensive biological activity that may be responsible for increase in hydrophobic character and liposolubility of supramolecular topologies of OMC-Bi(V) and OMC-Co(II) ultimately enhanced biological activity.

Keywords: Organic metal complexes; molecular modeling; XRPD; quantum structures; Bi(V); Co(II)

INTRODUCTION

One class of ligand that has stimulated continuing interest in a wide range of areas for nearly thirty years which are known as i.e.

antibiotic drugs. This research area is of a tremendous interest for researchers because it is exploring new ligand environments for transition and main group metal. This is well known branch of chemistry in which several pathways were used for the development of new synthetic mimics for biological systems. The chemistry of such ligands complexes, in general, represented a vast research area of chemistry, biochemistry and biomedical sciences.^{1,2}

Coordination compounds of different metal ions of polyamines containing antibiotic drugs have applications in medicine and catalysts. Their importance as model systems in bioinorganic

*Corresponding Author: Dr. Rajiv Kumar
Tel: +91-9810742944
Email:chemistry_rajiv@hotmail.com

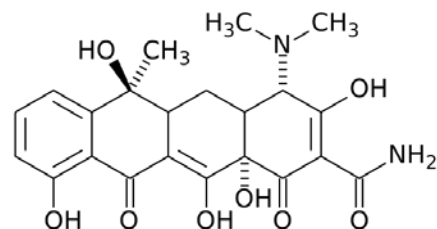
Cite as: *J. Integr. Sci. Technol.*, 2016, 4(2), 96-106.

©IS Publications ISSN 2321-4635 <http://pubs.iscience.in/jist>

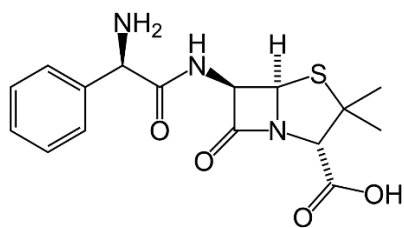
chemistry is a new research area. Metal ions play a key role in the physiological action of antibiotic drugs.

Main group or transition metal elements are involved in specific interactions with antibiotics, proteins, membrane components, nucleic acids, and other biomolecule.^{2,3} These interactions has facilitated the synthesis of metal nanoparticles by using naturally occurring biomolecules.⁴ The use of antibiotic drugs as ligands has attracted increased attention recently because of their importance in biological, synthetic, and industrial processes.

Many drugs possess modified toxicological and pharmacological properties when they are used in the form of metal complexes.⁵⁻⁹ These results encouraged us to investigate the coordination chemistry of antibiotics with transition and main group metal ions. In this study, an attempt to examine the modes of binding in the solid state and to study biological activity. In continuation of our work on metal interactions with antibiotic drugs,¹ in order to explore this research area, we have used some antibiotic drugs for synthesizing the novel class of metal complexes.



(a) Tetracycline



(b) Ampicillin

Figure 1. Molecular structure of antibiotic drugs used as ligand (L) and mixed ligands (ML)

Supramolecular topologies of organic metal complexes i.e. OMC-Bi(V) and OMC-Co(II) were derived from ML (mixed ligand)/ L (ligand); ML is the mixer of tetracycline, [2-Naphthacene-carboxamide, 4-(dimethylamino)-1,4,4a,5,5a,6,11,12a-octahydro-3,6,10,12,12a-pentahydroxy-6-methyl-1,11-dioxo-, [4S-(4 α , 4a α , 5a α , 6 β , 12a α)], and ampicillin, (2S,5R,6R)-6-([(2R)-2-amino-2-phenylacetyl]amino)-3,3-dimethyl-7-oxo-4-thia-1-azabicyclo[3.2.0]heptane-2-carboxylic acid and L is only tetracycline i.e antibiotic drugs and further used to prepare its organic metals complexes with Bi(V) and Co(II). A complete set of spectral investigations, (IR, ¹H-NMR, ¹³C-NMR, and MS), physicochemical investigations (elemental analyses), X-ray powder diffraction and molecular modeling on binding capabilities of antibiotic drugs with Bi(V)/Co(II), were displayed to investigate binding patterns with O₂/ O₃ donor sets. The focus of

this article was on synthesis, physical studies, characterisation and metalloantibiotics effectiveness with concern their coordination and organometallic behaviour of OMCs. The organic metal complexes reported in this article constituted a new class of metal based antimicrobial agents and thus their metalloantibiotics were investigated.

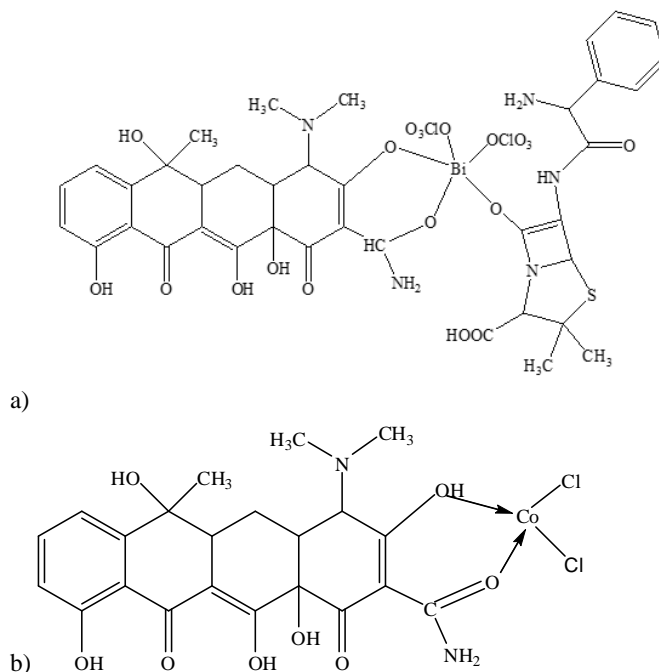


Figure 2. Molecular arrangement of OMCs

OMCs were screened against different plant pathogens i.e. *Aspergillus flavus*, *Candida albicans*, and *Candida glabrata*. On the basis of result and discussion, supramolecular architectures of organometallic assemblies of OMCs-Bi(V) and OMCs-Co(II), showing very good antimicrobial activities as per their corresponding pharmacophore geometries specified.

MATERIALS AND METHODS

All the chemicals and solvent used in this study were of analytical grade and used as procured from Aldrich and dried over 4 Å molecular sieves. Solvents were purified by standard procedures.¹⁰

Materials and Instruments

The stoichiometric analysis (C, H and N) of organometallic assemblies were performed using a Carlo-Ebra 1106 elemental analyzer. Metal content was estimated on AA-640-13 Shimadzu flame atomic absorption spectrometer in solution prepared by decomposing the respective complex in hot concentrated HNO₃. IR spectra were recorded on a Perkin-Elmer FTIR spectrometer in KBr. The electronic spectra were recorded in water on a Beckman DU-64 spectrometer with quartz cells. ¹H and ¹³C NMR spectra were recorded at ambient temperatures on Bruker AMX400 and DRX500 spectrometers with TMS as internal reference and D₂O as solvent. Chemical shifts (δ) were expressed in parts per million (ppm) relative to (TMS) tetramethylsilane. The crystals needed for

X-ray diffraction analysis were tried to produce three dimensional crystalline models as follows: one gm of OMC-Bi(V) or OMCs-Co(II) was dissolved at 40 °C in minimum amount of methanol. A clear solution was obtained and heated for 4 to 5 minutes under reflux and was then filtered off at a high temperature. The solution was cooled down to room temperature and closed with a semipermeable membrane so that methanol cannot evaporate but still a very slow evaporation was there. The mixtures were stored at room temperature for a period of three to five weeks. Very small crystals were filtered off and dried.

Bio Assay

The free ligands, mixed ligands and supramolecular topologies of organometallic assemblies (OMCs-Bi(V) and OMCs-Co(II)) were tested against various bacterial strains with the agar well diffusion method. The antifungal activity against various fungi was also tested and the results are presented as comparative manor graphically.

Hanging Drop Method-Antifungal Activity

The concentration of test compounds was 500 ppm used to study the antimicrobial activities on germination of fungal spores by hanging drop method. The germination of spores was observed under microscope after 8 hours of incubation at 30°C for incubation period 6-9 days. The percentage inhibition of spore germination was calculated as follows, % Inhibition of spore germination = Total number of germinated spore/ Total number of spore¹¹.

XRD Measurements

XRD powder patterns were recorded on a vertical-type Philips 1130/00 X-ray diffractometer, operated at 40 kV and 50 mA generator using Cu-K α line at 1.54056 Å as the radiation sources. Sample was scanned between 5° to 70° (2 θ) at 25 °C. Crystallographic data was analyzed using CRYSFIRE-2000 powder indexing software package and the space group was found by CHECK CELL programme. Debye-Scherrer relation was derived with the help of 100% peak width to determine the particle size. Experimental density was observed through Archimedes method.

Molecular Modeling

The correct sequence of atoms in three dimensions was obtained to get reasonable low energy molecular geometries. The molecular modeling described application of classical mechanics to determine molecular equilibrium in proposed molecules Emphasize were taken on molecular structures of ML/L and organometallic assemblies help us to understand mechanism of biochemical transformations and in designing new methodologies to get perfect molecules for such purpose. 3D molecular models of organometallic assemblies were created using CS Chemdraw 3D program package. The correct stereochemistry was assured through manipulation and modification of molecular coordinates to obtain reasonable low energy molecular geometries. The optimized structures of OMCs were performed by MM2. The potential energy of molecule was sum of following terms: $E = E_{str} + E_{ang} + E_{tor} +$

$E_{vdw} + E_{oop} + E_{ele}$. where all E's represent energy values and found corresponds to given types of interaction. The subscripts str, ang, tor, vdw, oop and ele denote bond stretching, angular bonding, torsion deformation, vander waals interactions, out of plain bending and electronic interaction respectively.

General Procedure For Synthesis of OMCs

Preparation of Solutions (Ligand and Mixed Ligand)

A required amount of corresponding antibiotic drugs/drug were mixed in 1:1 ratio in equimolar amount and dissolved in CH₃OH.

Preparation of Bi(V) And Co(II) Solution

Sodium bismathate was dissolved in 1:1 HClO₄ or 0.1 M H₂SO₄ respectively as source of Bi(V) and CoCl₂ for OMC-Co(II). The transparent filtrate was obtained as metal salt, further used for complexation. Bi(V) solution was prepared by drop-wise addition of metal salts solution to 100 ml of 0.01 M Bi(V) solution in methanol with continuous stirring at room temperature. The pH of the solution was adjusted by drop-wise addition of NaOH in the range of 2-3 using a pH-meter separately.

General Method for Synthesis of OMC-Bi(V) and OMC-Co(II)

Organic metal complexes of Bi(OCIO₃)₅ or CoCl₂ was prepared by dissolving equimolar amounts of mixed ligand/ligand (ML, gm, 0.5 mmol)/(L, gm, 0.5 mmol) and solution of Bi(OCIO₃)₅ (gm, 0.5 mmol) or CoCl₂ (gm, 0.5 mmol) respectively in minimum quantity of CH₃OH (20 cm³, absolute) in 100 ml round bottom flask. The mixture was heated for 6 h, until volume was reduced to half original at ~82-85 °C on a water bath. A solid mass separated out on cooling at ~5 °C was refrigerated for better crystallization. It was then filtered, washed with CH₃OH and dried over P₂O₅ in vacuum. The formed crystals were re-dissolved for re-crystallization in excess amount of warm methanol. The clear solution obtained was left undisturbed for weeks to get very small fine crystals.

RESULTS AND DISCUSSION

Physiochemical Investigations

The reaction of mixed ligand (ML) with Bi(V) and ligand (L) with Co(II) afforded light crystals of organometallic assemblies in good yields. The product shows partial solubility in acetone, methanol, ethanol and acetonitrile, while considerably soluble in polar aprotic solvents like dimethyl formamide (DMF), dimethylsulfoxide (DMSO), organic acids and pyridine. OMC-Bi(V) and OMC-Co(II) having characteristic color were stable in air and practically insoluble in water, ethanol, methanol, chloroform and hexane. After elemental analysis, organometallic assemblies of antibiotic drugs i.e. tetracycline and ampicillin under study were found to be monomeric in nature. A better insight of molecular structures achieved using topological analysis, i.e. using multidimensional approach of spectral investigations. In results and discussion, there was a network of tactics of spectral observations at molecular level help to understand molecular arrangements of OMC-Bi(V) and OMC-Co(II). Adjustability of concerned mixed ligand or connectivity or its selection abilities towards Bi(V) and Co(II) through specific coordination sites were explored. Elemental

analyses (CHN) obtained was satisfactory and matched accurately with stereochemistry of corresponding organometallic assemblies. Empirical formula were derived and assigned to each OMCs i.e. OMCs-Bi(V) and OMCs-Co(II) as per general composition¹². Elemental analyses were listed with proposed empirical formula in table 1.

Table 1. Elemental analyses (%) of analytical composition of OMCs; calculated/found

OMCs, Empirical Formula	C	H	N	Metal, Co/Bi
Co(L)(Cl ₂)	46.01	4.21	4.88	10.26
C ₂₂ H ₂₄ CoN ₂ O ₈ Cl ₂	(45.91)	(4.11)	(4.56)	(10.10)
Bi(ML)OClO ₃	38.10	3.53	5.83	17.40
C ₃₈ H ₄₂ BiN ₅ O ₂₀ Cl ₂ S	(38.01)	(3.41)	(5.81)	(17.33)

IR Spectra of OMCs

Spectroscopic investigations, especially I.R. spectroscopy, helped to demonstrate structure of OMC-Bi(V) and OMC-Co(II) as well as binding abilities of ligands. Specially most important information about OMC-Bi(V) and OMC-Co(II), were observed from mixed ligands or simple pure ligand together by comparing IR spectra of both drugs used for complexation, and it was proved that their donor atoms working as a binding sites. But for OMC-Co(II), here, data available from only simple ligand, its data compared to the IR spectra of OMC-Co(II). So in OMC-Bi(V), it was difficult to find out binding sites compare to OMC-Co(II). It was quite interesting to see IR spectra of OMC-Bi(V) and OMC-Co(II), here most important IR bands were reported specially where was a shifting due to chelation during OMCs formation. Used spectroscopic techniques and their reported data gave a fine framework of their molecular structure of OMC-Bi(V) and OMC-Co(II), which further explored with the help of molecular modeling. After all some fine quantum structures were obtained further confirmed by XRPD observation.

In IR spectra of OMC-Bi(V) and OMC-Co(II) as well as ML/L showed the presence of free OH stretching in form of broad bands, were observed in the region ~3474, 3390 and 3392 cm⁻¹. A group of sharp and intense bands were observed at ~3245-3215 cm⁻¹ corresponding to free primary -NH₂ in both ligands, there was no change was observed in these bands after complexation¹³⁻¹⁷. It showed that there was no role of these groups on coordination with metal ions. Further in IR spectra of OMC-Bi(V) and OMC-Co(II), new bands were observed at ~525-528 cm⁻¹ assigned as $\nu(M-O)$, indicated that coordination of carbonyl O-atom to metal centre.¹⁸ Perchlorate presence were also observed in OMC-Bi(V) and OMC-Co(II) by the presence of Cl=O transformation.

¹H-NMR of OMCs

¹H NMR spectra of mixed ligands /ligand and OMCs were observed and compared to authenticate chelation. Difference was observed in -OH proton peaks and confirmed deprotonation followed by formation of OMCs. The ligands showed a complex pattern in region δ 8.15–6.90 ppm for aromatic protons, and same was observed in spectra of OMCs. A very strong singlet was

observed at δ 4.25-4.37 ppm due to triazole proton. The magnetic characteristic of (-OH) protons was not equivalent for ligands, and this behavior showed a different complex formation after metallation of free metal ion(s) with ML/L. During mononuclear OMC-Bi(V) and OMC-Co(II) formation, two signals observed earlier at 13.91 and 13.59 ppm in free ML disappeared completely, confirmed deprotonation of -OH groups and formation of OMCs were occurred¹⁹. This confirmed involvement of these hydroxyl groups in formation of new bonds with metal ion(s) and yielded OMC-Bi(V) and OMC-Co(II). ¹H NMR spectra of ligands showed singlet at δ 11.21–12.54 ppm, and same was also presented in spectra of OMC-Bi(V) and OMC-Co(II), confirmed the presence of carboxylic protons within Bi(V)/Co(II) architecture. Signals appearance due to secondary (-NH-) or primary (-NH₂) protons at the same positions in ligands and OMCs showed non-involvement of these groups in coordination. Methylene protons on carbon linked to -N= moieties recognize at δ 3.90-4.22 ppm. This signal was a singlet arise from nonequivalent methylene protons in OMCs. In general, OMCs obtained were found to exhibit no additional resonances confirmed neat and pure encapsulation.

¹³C NMR of OMCs

¹³C NMR spectral peaks of ML/L and OMCs along with possible assignments were presented. Experimental values of all carbons within all ligands and OMCs were reported and found as per architectural features of OMC-Bi(V) and OMC-Co(II). ¹³C NMR spectra of >C=O of ML appeared at 191.5 ppm, this peak belonged to those carbons attached with hydroxyl groups of ligands and other were appeared at 155.9 ppm¹⁵. The ¹³C spectra of hydroxyl phenyl moiety attached to metal ion(s) appeared at 129.1-115.2 ppm while some carbons appeared at 149.8 ppm due to electron-withdrawing effect metal towards hydroxyl groups at this position. ¹³C NMR spectra of all carbons of amino, phenyl and thiophene moieties of ligands appeared at 116.2-150.2 ppm.¹⁹ In the case of one part of ML, the spectra of different carbons appeared in an up-field direction as compared with other carbon atoms in phenolic moieties of OMCs due to bond formation of oxygen with metal ion(s).

Electronic Spectra of OMCs

The coordination behaviour of Bi(V) and Co(II) with ML/L has been investigated using electronic spectroscopy in solution. Electronic spectra of Bi(V)-OMCs showed two peaks at 319-325 and 451-457 nm assigned as ($\pi \rightarrow \pi^*$) and ($n \rightarrow \pi^*$) transition respectively. OMCs displayed broad emission spectral transition indicating charge-transfer. The emission spectral features of OMC-Bi(V) and OMC-Co(II) were because of their ability of intra molecular energy transfer between triplet levels of ML, and L emitting energy levels of metal ion(s), which depended on energy differentiation. In organic solvents, the energy gap between ML triplet level and emitting level of Bi(V) may be in favor of energy transfer process. Because of it, OMC-Bi(V) and OMC-Co(II) displayed blue emission wavelength, and maximum emission peaks was shifted towards longer wavelength. It can be also seen that emission intensities of OMCs were stronger than ML/L.

Time-of-Flight (TOF) Mass Spectra of OMCs

Time-of-flight mass spectral displayed molecular ion species [M]⁺ and other peaks corresponding to fragmentation patterns of OMCs. The patterns of peaks in mass spectra reflect clear indication of successive degradation with a series of peaks corresponding to different fragments of OMCs. The intensities of reported peaks were directly related to stability of concerned fragments. Mass spectra of OMC-Bi(V) and OMC-Co(II), molecular ion peaks of concerned fragments (the ligand or fragments of the ligand with metal or metal + ligand) have been observed as MS (EI, m/z (%): 1198 (M⁺) and MS (EI, m/z (%): 573 (M⁺) as per their molecular formula.²² Mass degradation patterns proved the presence of isotropic ratio corresponding to metal ion(s) i.e. chloride and chlorate of Bi(V) and Co(II) along with ligands fragments. The results obtained were discussed to present breaking and demetallation patterns of OMCs. Mononuclear nature of OMCs was assigned as [M (fragments of the ligand)]⁺.

X-ray Power Diffraction Analysis of OMCs

XRPD spectra were obtained to study good quality of powder of OMCs. The density was determined by Archimedes method. Crystal methodologies (direct methods and Patterson synthesis) were utilized from XRPD data, all diffraction peaks were pointed out lead to extract intensities of a particular reflections. XRPD data was very good source to deduce accurate cell parameters of OMCs. The particle sizes of OMCs were calculated with the help of Debye-Scherrer equation. XRPD spectra of OMC-Bi(V) and OMC-Co(II) were presented to substantiate alignments in architectural features of OMC-Bi(V) and OMC-Co(II) and this confirmed the presence of metal(s) within OMCs frameworks. Crystalline nature of OMCs was confirmed from reflectance patterns. Indexing methodologies were performed using (CCP4, UK) the Crysfire program,⁵ with different crystal systems with varying space group. Merit of fitness and particle size of OMCs were derived from XRPD. The cell dimensions and other related parameters of OMCs obtained were shown in table 2 and this reveals crystalline nature of OMCs. GSAS programme for space group and density were performed by Archimedes method.

It was most important technique help us to understand the presence of metal in environment of both ligands. The indexing procedures were performed using (CCP4 UK) Crysfire program. Hence, powder X-ray diffraction pattern of all ligands and OMCs were recorded. The diffraction pattern revealed crystalline nature of OMC-Bi(V) and OMC-Co(II) for crystal system and GSAS program for space group and density were determined by Archimedes method.

Table 2. Crystallographic data of OMCs

OMCs	OMC-Bi(V)	OMC-Co(II)
Empirical formula	C ₃₈ H ₄₂ BiN ₅ O ₂₀ Cl ₂ S	C ₂₂ H ₂₄ CoN ₂ O ₈ Cl ₂
Formula weight	1200.7	574.17
Temp °K	298°	298°
Wave length (λ)	1.54056 Å	1.54056 Å
2θ range	12-80	16-50

Unit	a = 15.95464 (Å)	a = 14.27390 (Å)
Cell dimension	b = 15.95464 (Å)	b = 14.27390 (Å)
	c = 16.47710 (Å)	c = 9.51192 (Å)
	α = 90.00°	α = 90.00°
	β = 90.00°	β = 99.000°
	γ = 120.00°	γ = 120.00°
Volume (Å ³)	3632.32	1937.97
Crystal system	Tetragonal	Tetragonal
Space group	P422	P422
Density (g/cc)	1.08	1.47
Z	2	3
Index ranges	1 ≤ h ≤ 8	1 ≤ h ≤ 6
	0 ≤ k ≤ 5	0 ≤ k ≤ 1
	0 ≤ l ≤ 10	0 ≤ l ≤ 2
	M(9) = 6	M(11) = 10
	F(9) = 2	F(11) = 7
Avs. Eps	0.0000650	0.0000974
Particle Size (nm)	11.66	10.09

Molecular Modeling Parameters of OMCs

The energy-minimized model structures of OMC-Bi(V) and OMC-Co(II) were obtained, and specified to understand interconnected arrangements of atom i.e. bond lengths, bond angles and atomic coordinates of ligands and OMCs. This reported statistics have a good concurrence with XRPD data.

Table 3. Bond length of OMC- Bi(V)

No.	S. Atoms numbering and their location	Bond Distance [Å]
1.	Bi(57)-O(63)	2.1
2.	Bi(57)-O(58)	2.1
3.	O(56)-Bi(57)	2.1
4.	O(31)-Bi(57)	2.0
5.	O(29)-Bi(57)	2.1

Table 4. Bond angles of OMC-Bi(V)

No.	S. Atoms numbering and their location	Bond Angle [°]
1.	O(58)-Bi(57)-O(56)	145.8
2.	O(58)-Bi(57)-O(31)	164.0
3.	(58)-Bi(57)-O(29)	124.1
4.	Bi(57)-O(56)-C(43)	120.0
5.	Bi(57)-O(31)-C(28)	99.84
6.	Bi(57)-O(29)-C(17)	109.5

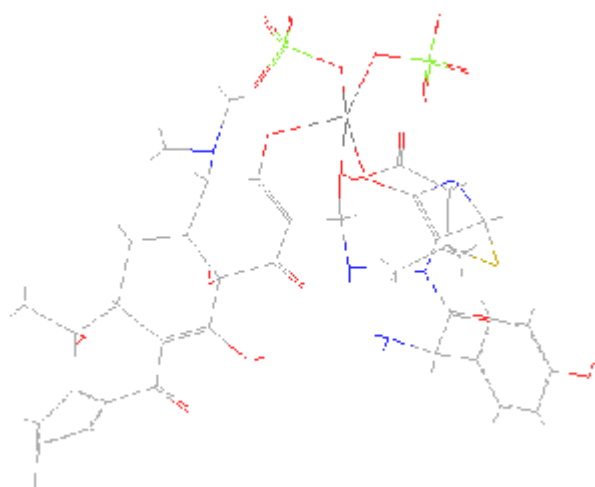


Figure 3. Stick-structure of OMC Bi(V)

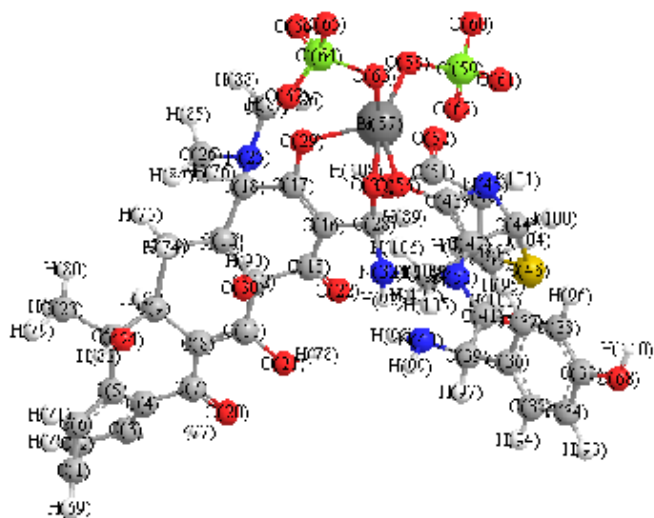


Figure 4. Optimized structure with HOMO of OMC- Bi(V); Color Code: C, Blackish Grey; N, Blue; O, Red; Bi, Dark Grey, Cl, Green and S, Yellow.

13	C	-1.8436	0.6416	1.4754
14	C	-2.6417	1.9387	1.4792
15	C	0.3975	-0.2835	1.1239
16	C	0.2259	-0.6652	-0.1606
17	C	-1.0143	-0.6245	-0.6585
18	C	-2.1742	-0.1730	0.1733
19	O	-0.8271	2.3774	7.6506
20	O	0.5397	1.8345	5.4844
21	O	1.2300	0.9627	3.4094
22	O	1.1011	-0.8931	1.8937
23	C	-3.6972	4.4748	3.2087
24	O	-1.5868	4.6904	2.2652
25	N	-2.9057	-1.3459	0.5698
26	C	-4.0767	-0.9534	1.3064
27	C	-3.2994	-2.0829	-0.6005
28	C	1.3837	-1.1291	-0.9884
29	O	-1.3420	-0.9867	-1.9224
30	O	-0.0499	2.0220	0.6611
31	O	1.0482	-1.0518	-2.3474
32	N	2.5237	-0.2920	-0.7285
33	C	9.8504	1.0921	-4.7365
34	C	9.9857	1.4058	-3.4439
35	C	8.9121	1.4375	-2.6477
36	C	7.7032	1.1554	-3.1441
37	C	7.5678	0.8417	-4.4367
38	C	8.6414	0.8100	-5.2329
39	C	6.5011	1.1909	-2.2526
40	N	5.5647	2.1623	-2.7501
41	C	5.8510	-0.1707	-2.2316
42	C	4.1083	-1.4489	-2.6021
43	C	2.7482	-2.0529	-2.5705
44	C	4.4957	-2.8949	-2.6021
45	N	3.0758	-3.2754	-2.6021
46	S	5.0634	-3.3172	-0.9307
47	C	3.4187	-3.3495	-0.1639
48	C	2.6928	-3.8815	-1.3188
49	C	3.3566	-4.2790	1.0409
50	C	2.9104	-2.0352	0.4138
51	C	1.2189	-3.6403	-1.1031
52	O	0.4591	-4.5759	-1.0231
53	O	0.7537	-2.3900	-1.0004
54	O	6.4731	-1.1311	-1.8443
55	N	4.6537	-0.3065	-2.6197
56	O	1.5262	-1.4694	-2.5225
57	Bi	-0.2045	-2.6583	-2.4897
58	O	-0.9987	-4.5804	-2.7809
59	Cl	-0.1375	-5.8931	-2.3425
60	O	-0.8704	-7.0521	-2.6335

S. No.) Atomic coordinates of OMC- Bi(V)

atom	x	y	z	
1	C	-1.1217	5.8791	6.4057
2	C	-2.0751	4.3323	7.4140
3	C	-1.3425	3.3562	6.8681
4	C	-1.1186	3.3457	5.5500
5	C	-1.6272	4.3115	4.7779
6	C	-1.6287	5.5782	5.2057
7	C	-0.3957	2.3772	4.9462
8	C	-0.7970	2.0609	3.6956
9	C	-2.1431	2.4986	3.2083
10	C	-2.2481	4.0151	3.3008
11	C	0.0257	1.3464	2.9209
12	C	-0.3553	0.9611	1.5254

61	O	1.0718	-5.9157	-3.0510
62	O	0.1264	-5.8404	-0.9668
63	O	-0.5518	-2.2085	-4.5113
64	Cl	-1.7937	-1.2388	-4.9288
65	O	-1.8213	-1.0875	-6.3222
66	O	-2.9983	-1.8117	-4.4978
67	O	-1.6296	0.0160	-4.3259
68	O	10.9384	1.0599	-5.5434
69	H	-0.4369	6.6713	6.7426
70	H	-2.8977	4.3207	8.1442
71	H	-2.0472	6.3728	4.5705
72	H	-2.8619	1.9823	3.8832
73	H	-2.1159	0.0321	2.3660
74	H	-2.3078	2.6473	0.6885
75	H	-3.7325	1.8565	1.2741
76	H	-2.7375	0.5345	-0.4754
77	H	-0.2945	1.6677	7.2537
78	H	1.8361	0.4430	2.8550
79	H	-3.7400	5.5848	3.2793
80	H	-4.1282	4.1486	2.2358
81	H	-4.2820	4.0273	4.0432
82	H	-1.5952	5.6319	2.2362
83	H	-4.0367	-1.3914	2.3287
84	H	-4.1132	0.1566	1.3801
85	H	-4.9861	-1.3213	0.7806
86	H	-2.8582	-3.1040	-0.5624
87	H	-2.9350	-1.5555	-1.5104
88	H	-4.4092	-2.1595	-0.6346
89	H	1.6285	-2.1827	-0.7262
90	H	-0.2278	1.9446	-0.2607
91	H	3.3132	-0.6073	-1.2921
92	H	2.7682	-0.3487	0.2601
93	H	10.9804	1.6379	-3.0355
94	H	9.0235	1.6957	-1.5842
95	H	6.5731	0.6096	-4.8451
96	H	8.5300	0.5518	-6.2964
97	H	6.8115	1.4697	-1.2207
98	H	4.7452	2.1872	-2.1433
99	H	6.0050	3.0822	-2.7640
100	H	5.2311	-3.2775	-3.3447
101	H	2.9476	-4.9628	-1.3867
102	H	2.3304	-4.2613	1.4714
103	H	4.0865	-3.9389	1.8093
104	H	3.6074	-5.3157	0.7228
105	H	3.6743	-1.2408	0.2582
106	H	1.9656	-1.7460	-0.0986
107	H	2.7199	-2.1581	1.5035
108	H	-0.1957	-2.2346	-0.8614

109	H	4.1130	0.5282	-2.9563
110	H	10.8400	0.8318	6.4832

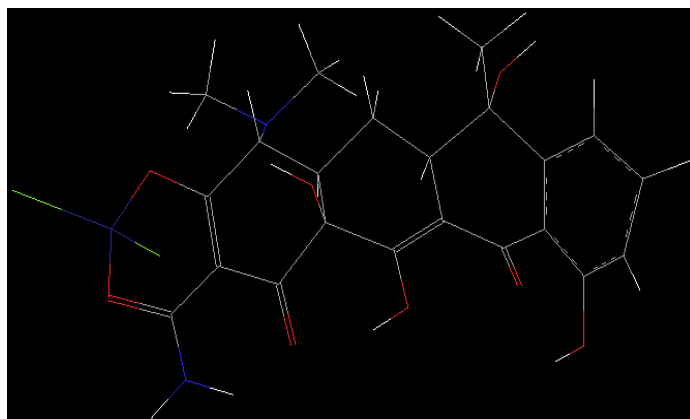


Figure 5. Stick-structure of OMC- Co(II)

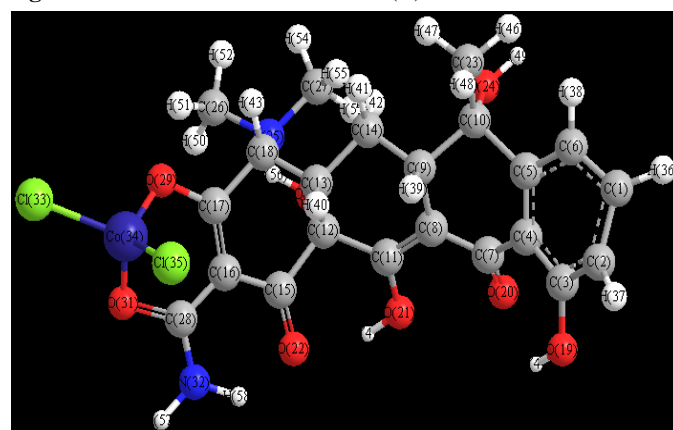


Figure 6. Optimized structure with HOMO of OMC-Co(II); Color Code: C, Blackish Grey; N, Blue; O, Red; Co, Dark Blue, Cl, Green and S, Yellow.

Table 5. Bond length of OMC- Co(II)

S. No.	Atoms numbering and their location	Bond Distance [Å]
	O(29)-Co(34)	1.4500
	O(31)-Co(34)	1.5006
	Co(34)-Cl(35)	2.1500
	Cl(33)-Co(34)	2.1500

Table 6. Bond angles of OMC- Co(II)

S. No.	Atoms numbering and their location	Bond Angle [°]
1.	Cl(35)-Co(34)-Cl(33)	115.7153
2.	Cl(35)-Co(34)-O(31)	104.4995
3.	Cl(35)-Co(34)-O(29)	104.4995
4.	Cl(33)-Co(34)-O(31)	107.2913
5.	Cl(33)-Co(34)-O(29)	107.2913
6.	O(31)-Co(34)-O(29)	117.9540

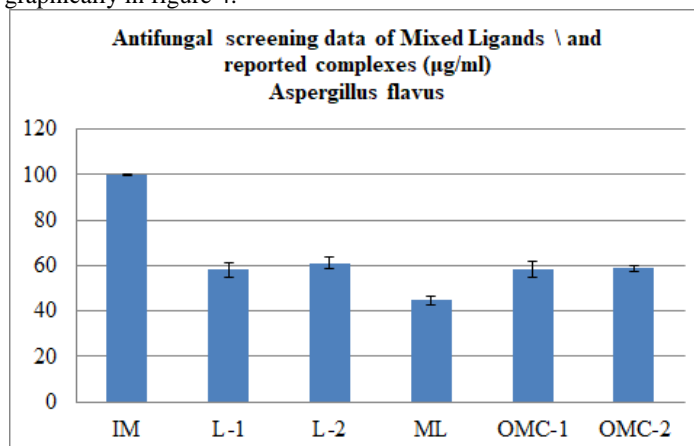
S. No.)	Atom	x	y	z
1	C	-3.9689	0.7356	2.6556
2	C	-4.0571	-0.6013	2.0225
3	C	-2.8992	-1.2698	2.0225
4	C	-1.7413	-0.6013	2.0225
5	C	-1.7413	0.7357	2.0225
6	C	-2.8551	1.4041	2.3391
7	C	-0.5441	-1.2272	2.0108
8	C	0.3644	-0.7060	1.1575
9	C	0.1732	0.6751	0.6125
10	C	-0.4716	1.5554	1.6751
11	C	1.4176	-1.4525	0.8096
12	C	2.4619	-0.9375	-0.1313
13	C	1.9312	0.2936	-0.8541
14	C	1.3720	1.2784	0.1642
15	C	2.7641	-1.9884	-1.1712
16	C	3.3685	-1.5287	-2.2886
17	C	3.6113	-0.2163	-2.3663
18	C	3.2293	0.7145	-1.2578
19	O	-2.8992	-2.6248	2.0225
20	O	-0.3038	-2.1817	2.7112
21	O	1.5425	-2.7016	1.3196
22	O	2.4865	-3.1538	-1.0161
23	C	-0.8298	2.9271	1.1189
24	O	0.3552	1.8252	2.7748
25	N	4.1577	0.6062	-0.1651
26	C	5.4695	0.9905	-0.6117
27	C	3.7416	1.4730	0.9042
28	C	3.7110	-2.3329	-3.3003
29	O	4.1984	0.3902	-3.4263
30	O	3.6159	-0.6208	0.5990
31	O	4.4398	-1.9418	-4.3736
32	N	3.3294	-3.5391	-3.2523
33	Cl	5.5466	0.2596	-6.0231
34	Co	4.1385	-0.4863	-4.5798
35	Cl	2.0748	-0.4439	-5.1815
36	H	-4.7453	1.1393	3.3221
37	H	-4.9861	-1.0051	1.5937
38	H	-2.8551	2.5041	2.3391
39	H	-0.4867	0.5774	-0.2784
40	H	1.1338	0.1738	-1.6213
41	H	1.1634	2.2621	-0.3128
42	H	2.0835	1.4800	0.9959
43	H	3.2414	1.7790	-1.5828
44	H	-2.0574	-3.1108	2.0225
45	H	2.3042	-3.2531	1.0735

46	H	-1.2974	3.5423	1.9199
47	H	0.0931	3.4320	0.7552
48	H	-1.5464	2.8097	0.2754
49	H	0.0390	2.3621	3.4812
50	H	6.1719	0.1375	-0.4787
51	H	5.4270	1.2711	-1.6879
52	H	5.8246	1.8599	-0.0144
53	H	3.5522	0.8690	1.8197
54	H	4.5428	2.2174	1.1108
55	H	2.8083	2.0031	0.6100
56	H	4.3749	-0.2809	0.1564
57	H	3.5795	-4.2001	-4.0289
58	H	2.7628	-3.8784	-2.4360

Refined models of OMC-Bi(V) and OMC-Co(II) displayed to find out sequence of new bonds formation between ML, L and metal Ion(s). There were a large number of deviations were noticed in distances, angles, or torsion and this happened because of specific electronic interactions. To ascertain architectural features of OMC-Bi(V) and OMC-Co(II), coordination abilities of ML/L with metal ion(s), with their molecular mechanics calculations were performed²⁴⁻²⁶. Energy-minimized models of OMC-Bi(V) and OMC-Co(II) were specified as bond lengths, bond angles, torsion angles and atomic coordinates of OMCs. Reported statistical findings were matched XRPD data. On the basis of this discussion, molecular models with HOMO were presented. XRPD results, related to crystal lattice and crystal size, illustrate relevance and molecular modeling data i.e. bond lengths, bond angles and bond coordinates also matched perfectly with propose geometries which were specified here. Related optimized models and ball scaffold were given in figures 3-6.

Antifungal Activity of OMCs

Antifungal activity of OMCs was reported against these pathogens i.e. *Candida glaberata*, *Candida albicans*, and *Aspergillus flavus* by the serial dilution method. MIC values and zone of inhibition (in mm) of OMCs were performed against fungi using Ketoconazole as standard. Results obtained were presented graphically in figure 4.



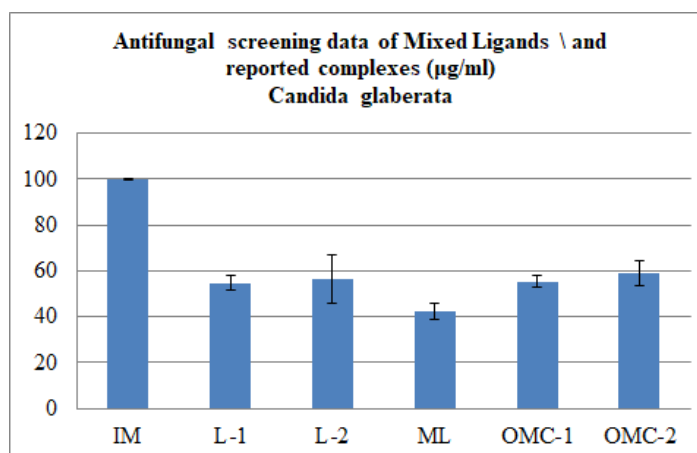
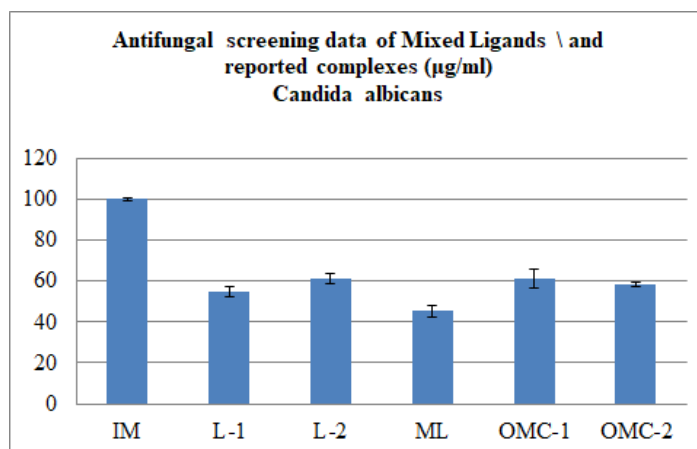


Figure 7. Graphical representation of antifungal activity OMC-Bi(V) and OMC-Co(II)

OMCs showed good biological activity. By making a comparison between biological activities of ligands and OMCs, it was pointed out that OMCs had moderate activity as compared all ligands. The higher inhibition zone of OMCs comparatively ligands can be explained on the basis of Overtone's concept and Chelation theory. On chelation, polarity of Bi(V) and Co(II) will be reduced to greater extent due to overlap of all ligands orbital. Because of this, partial sharing of positive charge of metal ion(s) and partial negative charge of donor atoms exchanged with each other. As a result, delocalization of π -electrons density clouds spread over surface of chelating ring. This enhanced penetration power of OMC-Bi(V) and OMC-Co(II) into lipid membranes and influenced binding sites of enzymes within microorganisms²⁷⁻²⁸. There were so many other aspect such as solubility, conductivity, dipole movement and bond length between Bi(V) or Co(II) and both ligands may influenced biological effectiveness of OMC-Bi(V) and OMC-Co(II). It was find out that in most cases OMCs were found to be more active than ligands. On the basis of reported results, a new methodology can be developed for designing of high standard antibacterial agents.

CONCLUSION

OMCs were prepared by using to different types of ligands from i.e. ML (mixed ligand) / L (ligand). Binding abilities of both ligands and other parameters were made by using various spectral analysis (electronic, vibrational, ¹H NMR, ¹³C NMR, and TOF-MS), physiochemical investigations (elemental analyses, X-ray powder diffraction) and molecular modeling, revealed coordination modes between Bi(V) and donor atoms. These spectroscopic techniques proved a better path way to observe stability and ability of both ligands to bind metals ion(s) by their donor atoms. Coordination ability of both ligands were discussed with Bi(V) and Co(II) metal used for chelation. Peaks shifting helped to find out molecular provision of considered metal based drug complexes i.e. OMC-Bi(V) and OMC-Co(II). It was noticed that coordinate performance in OMCs of Bi(V) and Co(II) have effected by using different stereochemistry ligands.

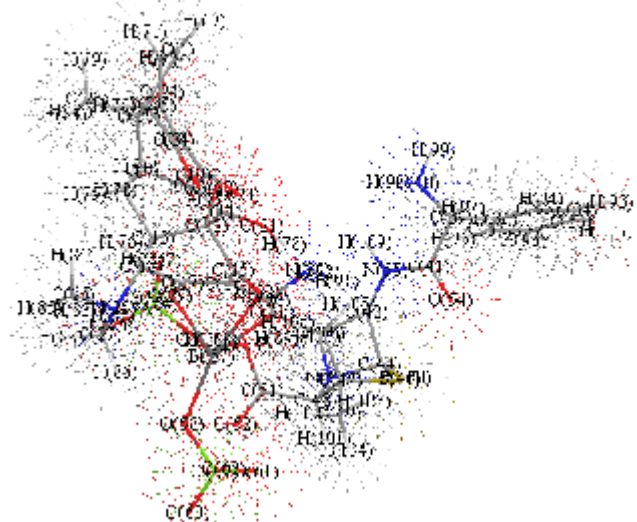


Figure 8. Charge density dotted structure of OMC- Bi(V)

Supramolecular topologies of metal based drugs of Bi(V) and Co(II), having different bonding atoms set for bonding, coordinate performance of Bi(V) ion(s) may be influenced by number of set for bonding atoms and their pharmacophore geometries specified as figures 8-9. Bi-bound and Co-bound with different groups came into existence because of bonding between O-Bi/O-Co and it further effected by the presence of -O- atoms of anions. These bonding between O-Bi or O-Co were at origin of moderate fungal efficiency detected for OMCs-Bi(V). To avoid any additional source of coordination expansion of Bi(V) atom, excepted for one caused by ML/L reaction components themselves.

Reported organometallic assemblies showed good biological activity. By making a comparison between biological activities of ligands and OMCs, it was pointed out that OMC-Bi(V) and OMC-Co(II) have moderate activity as compared ligands. The higher inhibition zone of OMCs comparatively ML/L could be explained on basis of Overtone's concept and Chelation theory. Due to interaction between aqueous Bi(V) or Co(II) (cations) and anionic constituents of fungal cell wall, metal uptake decreased and hence

toxicity decreased. But in case of OMC-Bi(V), and OMC-Co(II) since metal cations were already coordinated to ligands, it easily entered into fungal cells and hence exert higher metal toxicity. It has also been suggested that some electron set for bonding groups presented in ligands display extensive biological activity that may be responsible for increase in hydrophobic character and liposolubility of organometallic assemblies and ultimately enhanced biological activity of OMCs. There were so many other aspect such as solubility, conductivity, dipole movement and bond length between metal ion(s) and ligands may influenced biological effectiveness of these supramolecular topologies of OMCs.

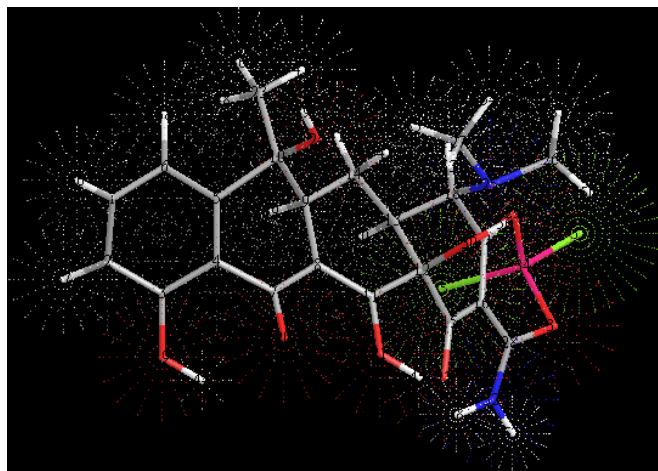


Figure 9. Charge density dotted structure of OMC- Co(II)

Spectral findings were compared peak by peak shifting to find out molecular provision of considered metal ion(s) in OMCs. A comparative analysis showed a higher antibacterial activity of OMCs than free ligands, mixed ligands and metal salt. OMC-Bi(V), and OMC-Co(II) exhibited moderate activities as compared with standard drug ciprofloxacin. It was also observed that OMCs were more potent fungicides than mixed ML or pure L.

This may support this argument that some type of bimolecular binding to metal ions or intercalation or electrostatic interaction caused inhibition of biological synthesis and prevented organisms from reproducing. The resistance mechanisms, therefore depended on which specific pathways were inhibited by drugs and alternative ways available for those pathways that organisms can modify to get a way around in order to survive. Resistance could be described in two ways: a) intrinsic or natural whereby microorganisms naturally did not possess target sites for drugs and therefore drug did not affect them or they naturally had low permeability to those agents because of differences in chemical nature of drug and microbial membrane structures especially for those that required entry into microbial cell in order to affect their action or b) acquired resistance whereby a naturally susceptible microorganism acquired ways of not being affected by drug.

The results indicated that OMCs have a good activity against all bacterial strains. The strong antimicrobial activities of OMCs against tested organisms suggested further investigation on these supramolecular topologies.

ACKNOWLEDGMENTS

One of the authors (Rajiv Kumar) gratefully acknowledges his younger brother Bitto for motivation. Authors acknowledge CSL Delhi University Delhi for providing computer facilities, I.I.T. Bombay and IIT Delhi for recording EPR and ^1H NMR spectra respectively.

REFERENCES

1. R. Johar, R. Kumar. Computational approach on architecture and tailoring of organometal complexes derived from streptomycin and Zn, Cd and Pb: antimicrobial effectiveness. *Appl. Organometal.Chem.* 2011, 25, 791-798.
2. B.S. Chhikara, S. Kumar, N. Jain, A. Kumar, R. Kumar. Perspectivity of bifunctional chelating agents in chemical, biological and biomedical applications. *Chemical Biology Letters*, 2014, 1(2), 77-103.
3. R.L. Carlin. *Transition Metal Chemistry* (Marcel ecker, New York) Vol. 1, 1965.
4. J. Singh, S. Kumar, B. Rathi, K. Bhrara, B.S. Chhikara. Therapeutic analysis of Terminalia arjuna plant extracts in combinations with different metal nanoparticles. *J Materials NanoScience*, 2015, 2(1), 1-7.
5. J.R. Anacona, C. Toledo. Synthesis and antibacterial activity of metal complexes of ciprofloxacin. *Trans. Metal Chem.* 2001, 26, 228-231.
6. Z.H. Chohan ZH, H. Pervez, K.M. Khan, C.T. Supuran CT. Organometallic-based antibacterial and antifungal compounds: transition metal complexes of 1,1'-diacetylferrocene-derived thiocarbohydrazone, carbohydrazone, thiosemicarbazone and semicarbazone. *J. Enzyme Inhib. Med. Chem.* 2005, 20, 81-88.
7. Z.H. Chohan, M. Arif, M.A. Akhtar, C.T. Supuran, Metal-Based Antibacterial and Antifungal Agents: Synthesis, Characterization, and In Vitro Biological Evaluation of Co(II), Cu(II), Ni(II), and Zn(II) Complexes With Amino Acid-Derived Compounds. *BioinorgChem Appl.* 2006, 83131, 1-13.
8. Z.H. Chohan, S.H. Sumrra, M.H. Youssoufi, T.B. Hadda. Metal based biologically active compounds: design, synthesis, and antibacterial/antifungal/cytotoxic properties of triazole-derived Schiff bases and their oxovanadium(IV) complexes. *Eur. J. Med. Chem.* 2010, 45, 2739-2747.
9. H. Neu. Cephalosporins in the treatment of meningitis. *Drugs*. 1987, 34, 135-153.
10. J.A. Riddick, W.B. Bunger. *Organic Solvents: Physical Properties and Methods of Purification* (3rd edn), Wiley: New York, 1970.; The crystals needed for X-ray crystal structure analysis were tried to produce but not succeed as follows: one gm of the bismuth OMC was dissolved at 40 °C in a very small amount of methanol as small as possible. A clear solution was obtained and heated for 4 to 5 minutes under reflux and was then filtered off at a high temperature. The solution was cooled down to room temperature and closed with a semipermeable membrane so the methanol cannot evaporate but a very slow evaporation was there. The mixtures were stored at room temperature for a period of three to five weeks. Very small crystals were filtered off and dried.
11. C.H. Collins, P.M. Lyre, J.M. Grange. *Microbiological Methods* (6th edn), Butterworth: London, 1989.
12. A.I. Vogel. *A Textbook of Quantitative Inorganic Analysis Including Elementary Instrumental Analysis*, fourth ed. Longman, London, 1978.
13. J. Coates. In: Meyers, R.A. (Ed.), *Encyclopedia of Analytical Chemistry: Interpretation of Infrared Spectra, A Practical Approach*. John Wiley and Sons, Chichester, 2000.
14. N.B. Colthup, L.H. Daly, S.E. Wiberly. *Introduction to Infrared and Raman Spectroscopy*. Academic Press, 1975, New York.
15. J.R. Ferraro. *Low Frequency Vibrations of Inorganic and Coordination Compounds*, 2nd edn. John Wiley: New York, 1971.
16. K. Nakamoto. *Infrared Spectra of Inorganic and Coordination Compounds*, 2nd Edn. (Wiley Interscience, New York) 1970.
17. L.J. Bellamy. *The Infrared Spectra of Complex Molecules*, 3rd Edn. (John Wiley, New York) 1971.
17. C.J. Ballhausen. *An Introduction to Ligand Field* (McGraw-Hill, New York) 1962.

18. E. Canpolat, M. Kaya. Studies on mononuclear chelates derived from substituted schiff base ligands (Part 4): Synthesis and characterization of a new 5-hydroxysalicyliden-P-aminoacetophenoneoxime and its complexes with Co(II), Ni(II), Cu(II) and Zn (II). *Turk. J. Chem.***2005**, 29, 409-415.
19. F.W. Wehrli, T. Wirthlin, Interpretation of Carbon-13 NMR Spectra, Heyden: London, 1980
20. A.B.P. Lever. Inorganic Electronic Spectroscopy. Elsevier, Amsterdam, 1984.
21. R. Kumar, B.S. Chhikara. Organometallic assemblies: p-electron delocalization, m-bridging spacers, flexibility, lipophilic nature, bio-accessibility, bioavailability, intracellular trafficking pathways and antimicrobial assimilation. *J. Organomet. Chem.* **2015**, 776, 64-76.
22. R. Shirly, The Crysfire System for automatic powder indexing 2002.
23. B. Ren. Application of novel atom-type AI topological indices in the structure-property correlations. *THEOCHEM*, **2002**, 586, 137-148.
24. D.X. West, S.B. Padhye, P.B. Sonawane. Structure and Bonding 76. Springer: New York, 1991, 1.
25. J.J. Gajewski, K.E. Gilbert, J. McKelvey. Advances in Molecular Modeling, Vol. 2, D. Liotta, Ed., JAI Press, New York, 1990.
26. H. Gonzalez-Diaz, F.J. Prado-Prado. Unified QSAR and network-based computational chemistry approach to antimicrobials, part 1: Multispecies activity models for antifungals. *J. Comput. Chem.***2008**, 4, 656-667.
27. C. Hansch, T. Fujita. A method for the correlation of biological activity and chemical structure. *J. Am. Chem. Soc.***1964**, 86, 1616-1626. Hyperchem 6.0, 1993. Hypercube, Inc., Florida.